Analyst

Accepted Manuscript

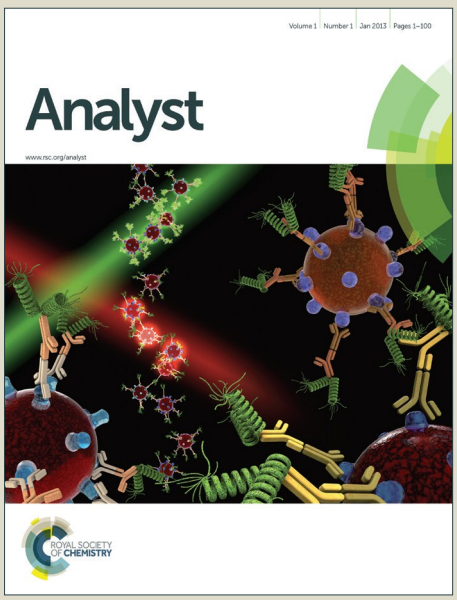

ROYAL SOCIETY OF CHEMISTRY

www.rsc.org/analyst

Analyst

ARTICLE

Study of Molecular Adsorption of Cationic Surfactant on Complex Surfaces with Atomic Force Microscopy

Received 00th January 20xx,
Accepted 00th January 20xx

DOI: 10.1039/x0xx00000x

www.rsc.org/

I. Sokolov,[a]† G. Zorn[b] and J.M. Nichols [c]

Study of molecular adsorption on solid surfaces is of broad interest. However, so far the study has been restricted to idealized flat smooth rigid surfaces which are rarely the case in real world applications. Here we describe a study of molecular adsorption on a complex surface of submicron fibers of a fibrous membrane of regenerated cellulose in aqueous media. We use a cationic surfactant, cetyltrimethylammonium chloride (CTAC) as the adsorbing molecules. We study the equilibrium adsorption of CTAC molecules on the same area of the fibers by sequential immersing the membrane in pure water, 1 mM and then a 20 mM solutions of CTAC. Atomic force microscopy (AFM) is applied to study the adsorption. The force-volume mode is used to record the force-deformation curves of the adsorbed molecules on the fiber surface. We suggest a model to separate the forces due to the adsorbed molecules from the elastic deformation of the fiber. Interestingly, knowledge of the surface geometry is not required in this model provided the surface is made of elastically homogeneous material. Different models are investigated to estimate the amount of adsorbed molecules based on the obtained force curves. The exponential steric repulsion model fits the force data the best. The amount of adsorbed surfactant molecules and its dependence on concentration are found to be reasonable compared to the data previously measured by means of Raman scattering done on a flat surface of silica.

Introduction

Adsorption of molecules on surfaces is important for basic understanding of surface chemistry processes. It is also central in such applications such as filtration, biosensing, and biochemical processing in which the adsorption surface is a compressible material of complex geometry. For example, polymeric membranes are used as physical barriers for virus filtration, as nutrient delivery systems for cell growth, or as fluidic platforms for *in vitro* diagnostic assays [1-3]. Interactions between membranes and biological systems are important parameters that impact every aspect of membrane performance. Phenomenological models prevail in filtration applications where membrane biofouling is the dominant challenge [4-6]. These models provide useful descriptions of the filtration behavior, but do not yield sufficient insight on *de novo* surfaces that improve performance. There are a number of challenges for in vitro diagnostic applications, such as fouling, non-selective protein capture, and poor reagent stabilization. Phenomenological models are limited in resolving these issues. The reliance on such models is due to the lack of methods that can characterize molecular adsorption to a topographically, mechanically, and chemically complex membrane surface. Despite its high importance, detailed characterization of surface adsorption in those applications remains an unmet need. From a fundamental point of view, it is interesting to learn the contribution of the surface geometry to the absorption properties. Here we describe a study that can address this challenge.

Plasmon-resonance [7], ellipsometry [8], optical spectroscopy [9], and atomic force microscopy [10, 11] (AFM) are used to detect molecular sorption to surface. However, these techniques do not allow measuring on rough or insufficiently flat surfaces [12, 13]. AFM is broadly used to image molecules directly on flat smooth surfaces [14-16]. AFM is also capable of measuring the interaction forces between the AFM probe and a surface, adhesion forces between specific molecules and a surface by determining the force required to detach a modified AFM probe from the surface of interest [17-19].

Molecules that are weakly adsorbed on a surface are extremely challenging to image with AFM. Another way to detect adsorbed molecules by AFM was suggested back in 1999[20]. It was demonstrated that AFM can be used to estimate the amount of the adsorbed molecules by analyzing force curves of deformation of the adsorbed layer. A similar approach was used to estimate the

[a] Departments of ME, BME, Physics, Tufts University, Medford, MA 02155, USA.
[b] Material Characterization & Chemical Sensing, General Electric Company, GE Global Research, One Research Circle, Niskayuna, NY.
[c] Membranes and Separations Technology, General Electric Company, GE Global Research, One Research Circle, Niskayuna, NY.
† Corresponding author: igor.sokolov@tufts.edu

Electronic Supplementary Information (ESI) available: AFM images showing the area of the measurements and areas of imaging artifacts. See DOI: 10.1039/x0xx00000x

amount of antibodies adsorbed on a flat polystyrene surface [12]. It should be noted that this approach is different from popular force spectroscopy studies [21-23]; it is based on the use of the approaching (rather than retracting) part of the force curves. Straightforward application of this method to a non-ideal, compressible surface is impossible because of the complexity of the force signal. A signal derived from a non-ideal compressible surface contains information about both the molecular layer and the substrate surface deformation, all within a complex geometry.

In the present work, we describe an AFM method allowing to measure adsorption of molecules onto non-ideal, compressible submicron fibers of a realistic (commercially available) cellulose membrane. The method consists of two steps. In the first step, the force-deformation curve obtained by AFM is separated into the deformation of the substrate and forces due to the adsorbed molecules. In the second step, the derived forces due to the adsorbed molecules are analyzed with the existing models to evaluate the amount of adsorbed molecules. We demonstrate the application of this method to measure absorbance of small molecules of cetyltrimethylammonium chloride (CTAC) on the surface of a cellulose membrane. The CTAC molecule was chosen as a test molecule which is relatively small in size (2.5nm, see Fig.S1), physisorbed on the surface of a cellulose membrane which is commonly used for biosensing and filtration applications. We found that the amount of adsorbed surfactant molecules was rather close to the results previously obtained by means of Raman scattering done on a flat surface of silica. The nature of the similarity is discussed.

Experimental Section

Chemicals

Cetyltrimethylammonium chloride (CTAC, Sigma-Aldrich) was used to test our model and to demonstrate the AFM ability to detect adsorption of organic molecules. CTAC is a cationic molecule, and therefore it should have electrostatic adhesion with the surface of the membrane, which is weakly negatively charged in pure water. It is close-to-linear molecule of 2.53 nm in length. This makes this molecule rather challenging to develop the AFM method to detect molecular adsorption on individual fibers of the filter membrane. Aqueous solutions of CTAC were used in the concentration of 1mM and 20mM (for comparison, the critical micellar concentration of the surfactant is 5mM). MilliQ ultrapure water of 18 MΩ was used as a medium for the imaging.

Atomic force microscope

A Dimension 3100 AFM (Nanoscope V controller) was used in this study. V-shaped DNPS standard narrow 200 μm AFM cantilevers with Veeco integrated pyramidal tips were used both to image the surface (when working in the contact mode) and to collect probe-surface interaction force curves to detect adsorption onto the membrane fibers (when working in the force volume mode). A spring constant for the cantilever of 0.098N/m was found using the thermal tuning method (the relative error of 10-20%); the radius of the AFM probe apex was estimated to be 20 nm by scanning a tip-check sample.

The following parameters were used during imaging in contact mode in liquids. Total signal on the AFM photodetector was set to 3 to 4 V, whereas the setpoint -0.5 to -1 V was used for imaging. The scan rate was set at 2 to- 3 Hz to optimize the image quality. Each image was collected in resolution of either 512 x 512 or 256 x 256 pixels.

The following parameters were used during imaging in force-volume mode in liquids. The initial scanning parameters were the same as described above. The cantilever deflection was set to 50 nm with the relative trigger option enabled. Force ramping speed was 3 Hz for a ramp size of 500 nm. The images were recorded with 16 x 16 up to 64 x 64 pixel sizes and 1024 points per force curve.

Membrane mounting for AFM study

Whatman RC-60 regenerated cellulose membranes with a 1 μm nominal pore size were used in this study. A 5-min two-component epoxy glue by Araldite was mixed as instructed, and allowed to cure for 2-3 minutes before using to mount the membrane. A small drop of semi-rigidified epoxy described above was mechanically smeared over the surface of silicon wafer. A small piece of the membrane was mounted on the top of semi-rigidified epoxy droplet described above. A silicon wafer with the attached piece of the membrane was used for the AFM measurements.

Electron microscope

A Phenom tabletop SEM working in backscattered mode was used to image membranes. Due to the use of backscattering electrons, no special preparation of the membrane was required. A piece of membrane was attached to a carbon conductive sticky tape, which was in turn mounted in a charge-reduction SEM sample holder.

Model to find the amount of molecules adsorbed using AFM data

AFM has been used to study molecules sorption in a host of literature. The force curves responsible for deformation of the molecular layers, and the ways to translate those curves into the amount of molecules observed on the surfaces were studied in [20]. The major difference in our case is the presence of non-flat

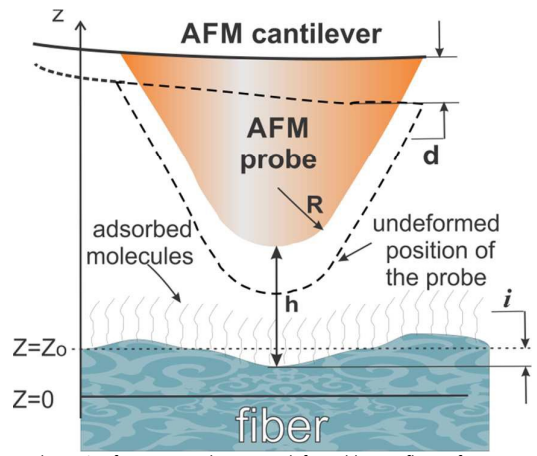

Fig. 1. A schematic of an AFM probe over a deformable non-flat surface covered with adsorbed molecules. Z is the relative piezo position of the cantilever, d is the cantilever deflection; Z_0 non deformed position of the sample; p deformation of the sample; Z=0 is for the maximum deflection assigned by the AFM user. h is the separation between the sample and AFM probe.

deformable substrate. Here we describe a model that neglects the assumption of flatness and incompressibility of the substrate. This model will allow us to separate mechanical deformation of the substrate from the forces due to the molecules absorbed on the substrate. It should be noted that this model is methodically similar to models developed for deformation of biological cells [24, 25]. Therefore, we will refer to those works when discussing some feature of the model presented here while focusing on the features of the present model which are different.

Figure 1 shows a schematic of an AFM probe interacting with a typical surface of membrane fiber, which is covered with molecular layer of adsorbed molecules. Both mechanical deformation on the substrate and long-range force cause the deflection of the cantilever d. The load force F is described by the Hooke's law, $F = kd$, where k is the spring constant of the AFM cantilever. Z is the vertical position of the cantilever shown in Figure 1. It is typically assumed that Z=0 for the maximum allowable deflection d_{max} (this can be assigned by the AFM user). $Z = Z_0$ is non-deformed position of the sample and p is the deformation of the substrate at the point of contact; h is the separation between the substrate and AFM probe. From the geometry presented in Figure 1, one can see the following relation between the parameters described:

$$h = Z - Z_0 + i + d \qquad (1)$$

AFM allows collecting parameters Z and d (called "raw data") directly. For the case of an AFM probe of well-defined geometry, e.g., a spherical probe and homogeneous isotropic material, we can use a particular case of the Hertzian model [26] to describe deformation, i as the function of load force $F=kd$

$$i = \left[\frac{9}{16}\frac{kd}{E}\sqrt{\frac{R+R_s}{RR_s}}\right]^{2/3} \qquad (2)$$

where R_s is the radius of curvature of the substrate at the point of contact (the Poisson ratio was chosen to be equal to 0.5 for simplicity).

Combining eqs.(1) and (2), one can write the following formula

$$h = Z - Z_0 + \left[\frac{9}{16}\frac{kd}{E}\sqrt{\frac{R+R_s}{RR_s}}\right]^{2/3} + d\,. \qquad (3)$$

Because Z is defined as zero when $d=d_{max}$, we can exclude Z_{0i} from eq. (3):

$$Z = \left[\frac{9}{16}\frac{k}{E}\sqrt{\frac{R+R_s}{RR_s}}\right]^{2/3}(d_{\max}{}^{2/3} - d^{2/3}) + (d_{\max} - d) + h. \qquad (4)$$

As shown previously [25, 27], the unknown parameters E and h can be found by using the following procedure. We assume that the maximum force developed by the cantilever (equals to kd_{max}) is sufficient to almost completely "squeeze" the molecular layer formed between the AFM probe and the substrate surface. This implies $h \approx 0$ at that maximum force. This assumption relies on smaller stiffness of the molecular layer forces compared to the stiffness of the surface substrate. This seems to be true for the solid polymer material of the fibers. It certainly depends on the value of d_{max}. It has to be sufficiently large to ensure enough load force to squeeze the adsorbed molecules. The assumption of $h = 0$ can be checked post-factum, after the parameters of the molecular layer being derived, to estimate the error due to this assumption. It is obvious that the effective stiffness of the molecular layer is increasing with the layer compression. At one point, the stiffness of the substrate becomes equal to the stiffness of the squeezed molecular layer, and therefore, their deformation responses become similar. Therefore, the error due to the deviation h from zero can be assigned to the uncertainty in the indentation depth. For example, if we consider 90% deformation of the molecular layer as a good approximation of completely squeezed layer, the error of 10% would result in maximum error of 1 nm for a maximum indentation depth of 10 nm. This is quite acceptable for the present degree of quantitative analysis (the maximum of 15% error in definition of the elastic modulus, E).

This approach allows to derive the molecular forces due to the adsorbed molecules unambiguously as well as the Young's modulus of the substrate. The Young's modulus E of the substrate is to be found assuming $h=0$ around the point maximum load. Using Equation (4), it can be written as

$$E = \frac{9}{16}k\sqrt{\frac{R+R_s}{RR_s}}\left(\frac{d_{\max}^{2/3} - d^{2/3}}{Z - d_{\max} + d}\right)^{3/2} \approx \frac{3}{8}\sqrt{\frac{2}{3}}kd_{\max}^{-1/2}\sqrt{\frac{R+R_s}{RR_s}}\left(\frac{d_{\max} - d}{Z - d_{\max} + d}\right)^{3/2}\Bigg|_{d\to d_{\max}} \qquad (5)$$

It should be noted that in the case of inhomogeneous material substrate, or when the force data are noisy, the described above procedure is more complicated. The exclusion of Z_0 at one particular point (when $d = d_{\max}$) is not sufficient. It makes sense to exclude Z_0 from equation 3 by fitting the experimental data in the vicinity of $d = d_{\max}$. This way one can also check a possible dependence of the Young's modulus on the indentation depth. A self-consistent model should demonstrate independency of the modulus of the indentation depth, see [28] for more detail.

When the Young's modulus is defined as described above, one can find the force due to the layer of the adsorbed molecules by using the following equation

$$h(d) = Z - \left[\frac{9}{16}\frac{k}{E}\sqrt{\frac{R+R_s}{RR_s}}\right]^{2/3}(d_{\max}{}^{2/3} - d^{2/3}) - (d_{\max} - d) \quad . \quad (6)$$

Knowing the surface geometry is not required to derive the force due to molecular layer: the case of mechanically homogeneous substrate

Although possible, it is rather difficult to measure the exact geometry of the substrate surface directly under the AFM probe when collecting the force curves. Here we propose a simpler method. Specifically, we will show that the method of derivation of the molecular layer force given by Equations (7) or (9) does not require the knowledge of the geometry of the AFM probe-surface contact in the case of when the substrate is made of mechanically homogeneous material. In the case of contact of two spherical surfaces, deformation is defined by Equation (3). It is known (ref. [29] ch.1.9) that when two objects of finite sizes and curvatures touch each other, deformation i due to the load force $F = kd$ can be written as $i = const \cdot d^{2/3}$. In our method, the constant of proportionality is derived by fitting Equation (4) when $h = 0$. In the case of spherical vertical contact, $const = (9k/16E\,((R+R_s)/RR_s)^{1/2})^{2/3}$. This allows finding the Young's modulus. However, the exact formula for this *const* is not needed to derive the force resulted from the adsorbed molecules, which is derived with the help of Equation (6). In case where *const* is derived from the fitting, equation (6) for the molecular layer force can be written as

$$h(d) = Z - const(d_{\max}{}^{2/3} - [F/k]^{2/3}) - (d_{\max} - F/k). \quad (7)$$

One can see that the force due to molecular layer derived by equation (7) does not require the knowledge of the geometry of the AFM probe – surface contact. However, to quantify the derived force in terms of the density of adsorbed molecules (see, for example, Equation 8 later), the geometrical information of the contact is required. Certainly this information can be derived from AFM high resolution surface imaging. However, in the case of homogeneous material of the substrate, the required geometry (for example, the radius of the spherical surface contact, R_s) can be calculated from the fitted value of *const*. Thus, the geometrical information hidden in *const* can be used to calculate the parameters of the molecular layer.

To amplify, when dealing with mechanically homogeneous material, the effect of non-flat geometry studied under the AFM probe can be taken into account without the explicit measurement of the surface geometry. Within the scope of this work, it is an interesting observation. Because the used cellulose might have heterogeneous mechanical properties, the actual experimental verification of this part of the method is beyond the scope of the present paper. For the current work, we have always been able to find a sufficiently flat area, and thus, we demonstrate the method on such flat areas.

Modelling of the force curves as a function of the adsorbed molecules

It is worth noting that the force acting between the AFM probe and sample surface exclusively due to the adsorbed molecules, given by equation (6), is independent of the any information about substrate. Derivation of eq.(6) was free of the assumption about the nature of adsorbed molecules. There is essentially only one assumption used to derive this equation, the absence of noticeable horizontal components of the stress tensor acting on the substrate by the molecular layer (or the Poisson ratio close to zero)[24]. This is typically true when the interaction between molecules is weak (weaker than interaction with the substrate; otherwise, the molecules would form an elastic layer). This is conceivably correct for the adsorbed molecules, like the one considered in the present work, which do not create a solid coating.

To estimate the total amount of absorbed molecules, one needs to have a model describing the force between the AFM probe and sample surface due to the absorbed molecules. Such models were investigated in a number of works. Here we discuss a few such models.

There is a steric entropic component [30] to the force caused by overlapping steric repulsion between adsorbed molecules described by the Alexander-de Gennes model. Within this model, we assume that the adsorbed molecules can be treated as entropic grafted polymeric brush. A corresponding force of steric repulsion between the AFM probe and sample surface covered with such molecules can be found with the Derjaguin approximation [20, 25, 31]

$$F_{molecular} \approx 50 k_B T R N^{3/2} \exp(-2\pi h/L) L, \quad (8)$$

where h is the probe-surface distance, L is the equilibrium thickness of the brush, N is the surface density of the brush constituents (grafting density), R is the radius of the AFM probe, and T is the medium temperature. This exponential form is useful for numerical fitting of experimental data. The formula is a

good approximation for a limited interval of h: $0.2 < h/L < 0.9$.

In some cases the brush distribution can be characterized as double brush [32] with two different sets of parameters, N_1, L_1 and N_2, L_2. Because we are dealing with the averaged force curves, such a double brush distribution can be described by simple additive formula:

$$F_{molecular} \approx 50 k_B T R \begin{bmatrix} N_1^{3/2} \exp(-2\pi h / L_1) L_1 + \\ N_2^{3/2} \exp(-2\pi h / L_2) L_2 \end{bmatrix}. \quad (9)$$

Although it is unlikely to expect a large interaction between adsorbed CTAC molecules, we still consider a model in which the adsorbed molecules start forming an elastic (though soft) layer. Forces due to deformation of such a layer will be different from the one given by Equation (7). Such a case is rather easy to identify by a specific force response that is substantially different from eq.(7) [10, 25]. Assuming purely elastic response of such molecular layer, one should expect repulsion given by the Hertz model (in conjunction with the Derjaguin approximation):

$$F_{molecular}(h) = \frac{4}{3} E \sqrt{R}\, (L-h)^{3/2} \quad , \quad (10)$$

where h is the probe-surface distance, L is the size of the molecular layer, E is Young's modulus of the layer, R is the radius of the AFM probe, $0<h/L<1$. Again, here we assumed inconsiderable tangential stresses due to compression of this layer (zero Poisson ratio). This seems to be plausible for the surfactant layer physiosorbed on the cellulose surface.

If the molecular layers are continuous but sufficiently soft (characterized by the layer bending modulus K), then the molecular layers can induce repulsion due to undulation force (the entropic force arising from the confinement of thermal excited modes within a smaller region between the AFM probe and sample surface) [33]:

$$F_{molecular}(h) = \frac{3\pi^3 (k_B T)^2}{32 K h^3} R. \quad (11)$$

For the case of mobile chain polymers which can escape from under the AFM probe during indentation, the force dependence changes to $F_{molecular}(h) \sim h^{-2}$ [34].

Finally, the force due to electrical double layer has to be mentioned. Because the surface potential caused by the sorption of CTAB/CTAC surfactants was found to be quite large [35], one can use the weak overlap approximation [36]

$$F_{\text{Molecular}} = (128\pi R\, kT \rho_\infty / \kappa) \tanh[\frac{ze\psi_1}{4kT}] \times \tanh[\frac{ze\psi_2}{4kT}] \exp(-\kappa d) \quad , \quad (12)$$

where k is the Boltzmann constant, ρ_∞ is concentration of counterions far from the surfaces, ψ_1 and ψ_2 are the surface potentials of the AFM probe and sample surfaces, respectively, κ^{-1} is the Debye length, which is a measure of the thickness of the electrical double layer.

Results

The force-volume method was used to measure the force deformation curves, and simultaneously, to extract information about surface topology (though at limited spatial resolution). The knowledge of geometry is important for quantitative characterization of the adsorbed molecules because of two reasons: 1) as mentioned above, knowing the geometry is required in the case of mechanically heterogeneous substrate 2) even in the case of mechanically homogeneous substrate, the force curves should be recorded at the region free of artifacts.

The main challenge in applying force-volume AFM to analyze membrane is the complexity of the sample surface. Membrane materials are relatively soft with complex surface morphologies. Figure 2 presents an SEM image of the membrane showing *a complex network of submicron fibers*. Such fiber morphology is highly challenging for the AFM techniques and can preclude from obtaining any meaningful data because of three reasons. The AFM probe can easily penetrate between the membrane fibers and become entangled in the mesh. The fiber mesh may also be excessively soft and unstable under the pressure of the AFM probe. Finally, such a hydrophilic network of fibers can slowly absorb water, and continuously change its morphology, which makes the AFM imaging very challenging, depending on the speed of the sample expansion.

The force-volume technique has been recently demonstrated to detect protein-surface interactions in a number of applications. This technique has been applied to study the adsorption of bovine serum albumin (BSA) molecules onto naturally rough polystyrene surface of 96-well plates. [12] However, to the best of our knowledge, the force-volume AFM method was not successfully applied to such complex system as the membrane shown in Figure 2.

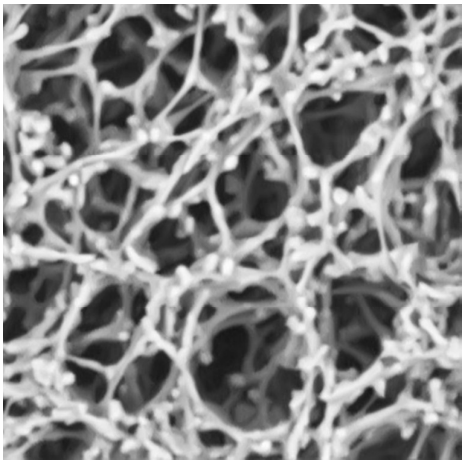

Fig. 2. A 16x16 micron SEM image of the cellulose membrane showing fibril morphology. This geometry represents a substantial challenge for AFM to study individual fibers.

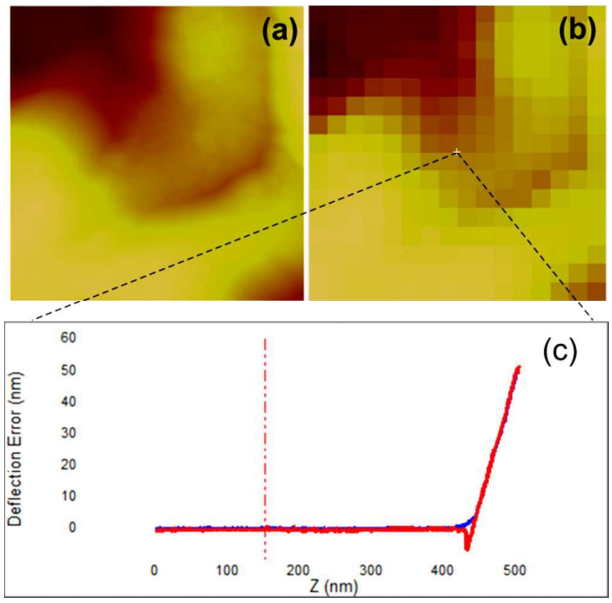

Fig. 3. Two-dimensional images of 2x2μm^2 area of the membrane, (a) imaged with AFM in contact mode, (b) imaged in the force-volume mode. (c) An example of a force curve recorded at a pixel of the membrane surface in the force-volume mode.

The key risks that were targeted in this study were: a) the ability to mount a membrane sample that is *stable* to AFM probing; b) the ability to find representative areas on the membrane surface where the force-volume AFM mode could be recorded without artifacts and c) measuring changes in the force curves associated with adsorption. Below we will demonstrate successful addressing all the above issues.

A relatively dull probe with a sufficiently large cone angle was used to overcome issues of penetration excessively deep into such challenging membrane as shown in Figure 2. Although it preserves the AFM cantilever from destruction, it can produce a number of artifacts due to mechanical interaction of the sides of the AFM dull conical probe with the surrounding fibers. Supplementary figure S2 shows an example of the membrane scanned with AFM in contact mode in water. This allows for easy identifying the artifacts caused by touching the sample with the probe side (Fig.S2a), and finding the good parts of the fiber suitable for the force study (Fig.S2b).

When using the force volume mode, a low-resolution image of the surface as well as the force versus probe-surface distance data at each pixel of the surface are collected simultaneously. Figure 3 shows an example of a 2 x 2μm^2 AFM image of the membrane (the same area as in Fig.S2b) as well as a low-resolution image of the same area obtained in the force-volume mode (Fig.3b). Geometrical resemblance to the height images obtained in both modes can be clearly seen. Figure 3c is an example for the force curve recorded at an individual pixel at the middle of artifact-free area at the middle of

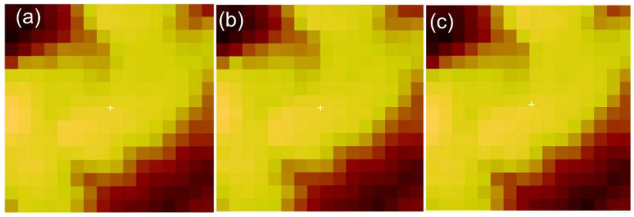

Fig. 4. Force-volume AFM images of the membrane imaged in (a) water, (b) 1 mM CTAC solution, (c) 20 mM CTAC solution. The time between images is approximately 35 minutes.

Fig.3. The deflection of the cantilever versus the vertical position of the scanner is the "raw data" that is recorded. The amount of adsorbed molecules can be found by modelling these raw curves as shown later.

The maximum load force was chosen to be adequately low to exclude any mechanical instability of the fibers. Therefore, scanning with AFM for both imaging and force measurements was sufficiently gentle to produce very robust scanning environment. To exclude swallowing the sample due to water absorbance, the sample was immersed in water for at least 30 minutes before starting imaging. To exclude a considerable thermal drift of AFM, the measurements were done after waiting for at least 6 hours after switching on the instrument. As we observed, same area of 3 x 3 μm^2 could be imaged continuously for at least three hours without a noticeable shift. Moreover, it was possible to change the media several times without moving the sample, Figure 4. This figure shows an example of sequential force-volume imaging of a membrane fiber immersed in different media. The left scan was taken in water. Then water was changed to a 1 mM aqueous solution of CTAC and a scan was taken after 30 minutes of equilibration. The solution was then changed again to 20 mM of CTAC and the surface was scanned again after 30 minutes of equilibration. Each scan required about 3 minutes and solution exchanges required about 2 minutes. So the time between each scan was approximately 35 minutes.

It should be noted that identifying the artifact-free areas by AFM imaging is obviously possible only when the AFM scanning of the fiber is stable. Otherwise, AFM

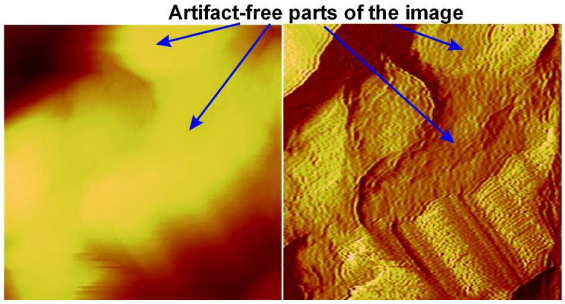

Fig. 5. Two-dimensional AFM images of the membrane scanned in water (the same as shown in figure 3). The left image is the height channel; the right image is the deflection (error) channel. The artifacts are clearly seen. The areas of the membrane surface to study adsorption of molecules are shown with arrows.

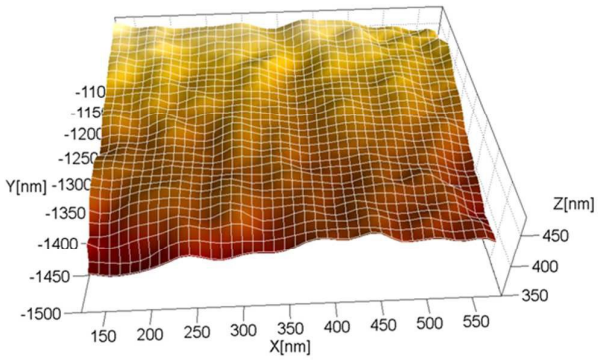

Fig.6. An example of sufficiently flat surface of the fiber. The force-volume analysis is done on this area. Mechanical homogeneity of the surface is not required by the model to extract the information about molecular adsorption for such a flat surface.

imaging of the surface after each force-volume study would be required. However, the AFM imaging could disturb the adsorbed layers, and therefore, such an artifact is avoided by collecting a high-resolution image using a simple contact mode only prior to adsorption of surfactant.

As we showed above, in the case of mechanically homogeneous substrate, the exact knowledge of the surface geometry is not needed to derive the amount of adsorbed molecules. However, mechanical homogeneity of cellulose fiber of study has not been investigated. Therefore, to avoid the potential influence of surface geometry, we measure the force curves due to the adsorbed molecules on a sufficiently flat part of cellulose fibers. Such areas were abundant on all fibers studied in this membrane. Figure 6 shows an example of a region with sufficiently flat geometry, which is a zoomed area of the top middle part of the fiber shown in figures 3-5.

Averaging of experimental data versus analysis of individual force curves

Complex surfaces of membrane fibers may have geometrically heterogeneous surfaces with different amount of molecules adsorbed. When studying such surfaces with AFM, it is needed to collect large data sets for statistical validation. In most cases processing each force curve separately is not required as it can be time- and resource- consuming. The analysis of averaged raw force data is a simple and time saving option, but also averages out the noise and measurement artifacts of the analyzed force curves. Averaging the raw data in the AFM method was studied in [37] in which it was found that the averaging gives very good estimation of the Young's modulus and relatively good averaged parameters of the brush (error <10-20%) if heterogeneity of the Young's modulus over the sample surface is less than 30%.

Figure 7a shows an example of raw data (the

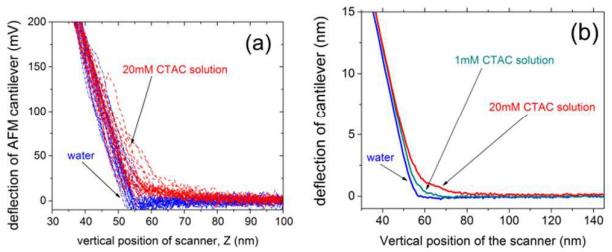

Fig.7. Representative raw data (the cantilever deflection vs vertical position of the scanner) collected over relatively flat areas of the fibers. a) 30 curves collected in water and 30 curves collected in the presence of 20mM concentration of CTAC surfactant; b) the averaged raw data curves collected in water, 1 mM and 20 mM of CTAC surfactant.

cantilever deflection d vs vertical position of scanner Z), collected over relatively flat areas of the fibers (30 curves collected in water and in the presence of 20mM concentration of CTAC surfactant). Although the overall increase of repulsion near the surface due to the adsorbed molecules of surfactant is clearly seen, the distribution of the force curves is rather broad. Force curves collected when concentration of CTAC surfactant was 1 mM would be hard to distinguish in this graph (not shown in Fig.7a. At the same time, it can be clearly seen it in the averaged data, Figure 7b, that the repulsion near surface is higher due to the adsorbed molecules at higher concentrations of surfactant.

Analysis of collected AFM force data

Figure 8 shows the analysis of the raw data obtained by fitting the experimental data with equations 4-6. The processed data are the average data collected in water (Figs. 8a,b), in surfactant of concentration 1mM (Figs. 8c,d), and in surfactant of concentration 20mM (Figs. 8e,f). Figs.8a,c,e show the fit using eqs.(4,5), which define the Young's modulus of the fibrous substrate. The values of the Young's modulus are summarized in Table 1. Figs.8b,d,f demonstrate the forces due to the presence of the adsorbed molecular layer.

We now analyze the forces the forces due to the presence of the adsorbed molecular layer. The analysis of forces in water and in 1mM surfactant solution is shown in Fig.9a,b. It is a clear short-range exponentially decaying function (a straight line in the log scale). Therefore, the power law (eq.11) and elastic layer deformation (eq.10) are clearly not good fits. In the case of 20 mM surfactant concentration, the exponential behavior is less obvious.

Figure 10 shows all three possibilities of fitting of the 20 mM force curve, the exponential, power law, and elastic layer repulsions. The power-law fitting, Fig.10b, shows the best fit for the power of 1.1±0.12. This excludes the undulation models which are required the power to be equal to 2 or 3 (eq.8). The attempt to fit these data with the elastic layer model (eq.11) is not good

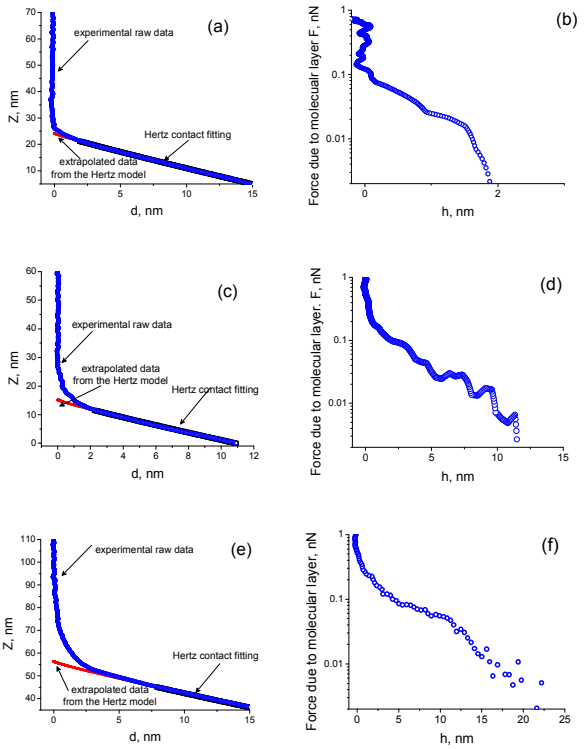

Fig.8. Fitting of the experimental data with equations (5-7) to derive the Young's modulus of the fiber and forces due to the presence of the adsorbed surface layer. The average data collected in (a,b) pure water, (c,d) in surfactant solution of concentration 1mM (e,f) in surfactant solution of concentration 20mM.

either. The best fit, Fig.10c, is attained when the power in the formula of equation 11 is equal to 4.0±0.2. This is too far from 3/2 implied by equation 11. Finally, the exponential fit (Fig.10a) shows the most reasonable matching the data. Thus, one can conclude that the exponential behavior seems to be the best fit of all force curves of interest. One has to note that the exponential behavior is observed due to the steric repulsion (eqs.8,9) and electrical double layer (12). As was demonstrated in [38], one can distinguish between these two forces by analyzing the slope of the force decay. Because we are working in pure water, the Debay length (the slope of the electrical double layer force) can be of the size of microns [39], which is much bigger than the observed here, Figs 9,10 (only a few nanometers). Secondly, if one still takes the Debay length value extracted from the fitting formula 12 would give an unrealistically high surface potential (>100mV). Such high potentials do not exist for regular materials. Therefore, we conceive that it is plausible to exclude the electrical double layer forces either. We will now process the force curves due to adsorbed molecules with the steric repulsion model (eqs.8,9).

Since the AFM probe is negatively charged in neutral pH [36], cationic surfactant molecules can also cover the AFM probe. Nevertheless, we do not expect this to be

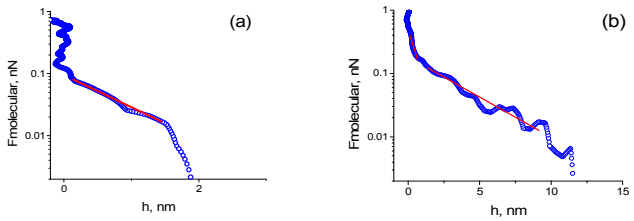

Fig.9. (a) Steric repulsion fitting for (a) water, (b) 1mM solution of CTAC.

considerable. As was shown [40], it requires several seconds for cationic surfactant to form a layer on silica surface. During the measurements, the AFM probe touches the surface 3 times per second. This should prevent the surface layer from forming.

The molecular forces in the surfactant concentration of 1 and 20 mM demonstrate double brush (eq.9) rather than single brush behavior (two exponential slopes). Nevertheless, if one ignores the small internal brush (presumably the same initial molecular roughness of the cellulose fiber which was observed in water with no surfactant present), and fits just the larger brush layer, the numbers for that large brush layer will not change substantially. The results of fitting the experimental data with both single and double brush (eqs. 8 and 9) are summarized in Table 1. The error is originated from variability of fitting (choice of the fitting regions).

Discussion

Despite the substantial difference in the forces observed for the different concentrations of the surfactant, the mechanical modulus of the substrate does not change substantially. This is an agreement with high stability of the membrane when changing surfactant concentration (figure 4). It should be noted that the modulus was measured around indentations of 4-9nm. Therefore, these are not the measurements of the macroscopic elastic modulus of the fibers. If this is the task, one should consider larger indentations. This has not been done here because it is beyond the scope of this work, which is to develop an AFM method to study adsorption of molecules on the membrane fibers.

The short-range force observed on the membrane fibers in water occurs due to either the surface roughness or the natural polysaccharide brush of the cellulose surface. More or less the same small and dense brush is observed in the surfactant solutions (when using the double brush model). Therefore, we assume that this brush does not have relation to the adsorbed surfactant molecules.

The size of the molecular brushes adsorbed in surfactant solutions (Table 1) indicates that the adsorbed surfactant formed multi-layered islands. This is because the brush size ranges between 23 to 50 nm (compare to 2.53nm of CTAC molecule) while the grafting density is

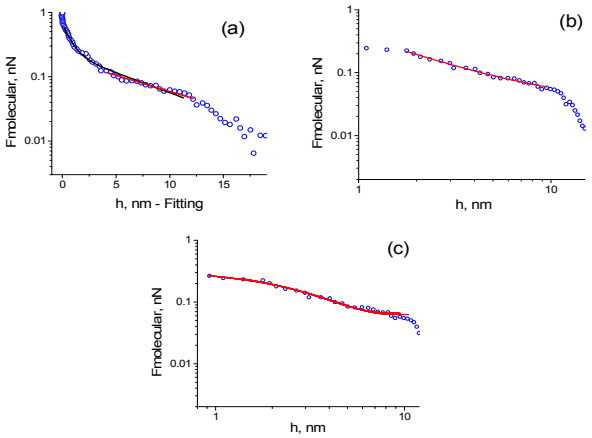

Fig.10. 20mM (a) Steric repulsion fitting. (b) power-law fitting, (c) Elastic layer fitting

smaller than the one needed for complete coating the surface (1.8 x10^6 μm^{-2}). This is in qualitative agreement with the individual force curves shown in figure 7a, in which one can see some time a break in the force curve, which is typically assigned to the break through a molecular layer [41]. This is also in agreement with the previous observation of growth of CTAC/CTAB layers on the surfaces of mica, silica, and graphite [9, 42]. These aggregates consist of micellar structures of surfactant molecules. The exact configuration near the surface depends on the substrate material, and presumably organized in cylindrical micelles for multilayered aggregates [42]. It should be noted that though the polymeric brush model shows the best fitting of the measured forces due to the adsorbed molecular layer, it is obviously an approximation for such a complex molecular layer. This could conceivably be explained by the physical structure of the layer, which has increasing density closer to the surface. The fact that the molecular density is similar to the one of the polymeric brush is interesting and presumably worth of further investigation.

To estimate the total number of molecules adsorbed to the substrate, we will use a rather simple assumption of linear (lamellar) structure of the surfactant layers. (It is conceivable to ignore the difference between the lamellar and hexagonal (nematic) packaging of cylindrical micelles as negligible compared to the approximate nature of the used steric repulsion models.) Then, the amount of molecules per unit area can be estimated as N_{surf}~N*L/L_0, where L_0 =2.53nm (the length of CTAC molecule forming the lamellar structure). It gives N_{surf}~(1-1.3)x10^5 μm^{-2} for 1mM and N_{surf}~(1.6-2.1)x10^5 μm^{-2} for 20mM (these results are shown in Table 1).

The obtained values of the adsorbed CTAC molecules were comparable to the previously reported results for adsorption of CTAB molecules (a sibling of the surfactant used in this work) on flat silica [9].

Table 1. Summary of the Young's modulus of the fiber, the length and grafting density of the molecular layer of surfactant adsorbed on the fiber.

	Modulus E (MPa)	Brush size, L (nm)	Grafting density, N (μm^{-2})	# of molecules (μm^{-2})
Pure water	25±4	4.5±1.2	(60±7)x10^3	N/A
1mM CTAC single brush	21±4	26±4	(10±1)x10^3	1.0x10^5
1mM CTAC double brush		2.0±1.0 23±3	(14±5)x10^4 (14±2)x10^3	N/A 1.3x10^5
20mM CTAC Single brush	18±5	50±10	(8±3)x10^3	1.6x10^5
20mM CTAC double brush		4.5±1.4 43±4	(86±8)x10^3 (12±3)x10^3	N/A 2.1x10^5

In that work, the adsorption was studied with Raman spectroscopy and the increase of the molecular concentration within ~100-200nm near the surface was measured. It was found that N_{surf} ~2.0×10^6 μm^{-2} for 1mM surfactant concentration and 3.1×10^6 μm^{-2} for 18mM (which is close to 20mM used in this work). Comparing these values with the results found here for cellulose fibers, one can see that amount of molecules adsorbed on cellulose is about 10 times smaller compared to the one on silica. This is quite expected because silica has the higher negative surface charge, which stronger attracts cationic surfactant molecules.

It is interesting to note that the ratio of the number of molecules adsorbed at 1 and 20 mM concentrations (equal to ~1.6) is virtually identical for cellulose and silica. At least partially, this could be explained by the fact that the surfactant molecules create multiple layers. This hides the original substrate for the subsequent absorption, making the further sorption substrate independent.

Conclusions

Here we demonstrated a method allowing to estimate molecular adsorption on a complex surface of submicron fibers of a fibrous membrane of regenerated cellulose in aqueous media. Surface of fibrous membranes are rather irregular at the nanoscale which precludes the use of regular AFM imaging modes to image individual molecules adsorbed on such surfaces. The force-volume AFM mode was previously used to record forces caused by the presence of the adsorbed molecules, and consequently, to calculate the amount of the adsorbed molecules. However, those methods were developed to estimate the number of molecules adsorbed on incompressible flat substrates. The novelty of our work is the in extension of that method to measuring molecules adsorbed on a non-flat compressible substrate. Our model reliably separates the deformation of the material of the soft membrane under the forces applied by the AFM

probe from the deformation of the adsorbed molecular layer. It was shown that the information about the surface geometry is not needed for deriving the parameters of the adsorbed molecules on an elastically homogeneous substrate. We demonstrated that the exponential steric repulsion model is the most plausible to explain forces due to the adsorbed molecules. The method was applied to study adsorption of cationic surfactant, cetyltrimethylammonium chloride (CTAC) on the surface of regenerated cellulose fibers. Adsorption data was collected over 2x2 μm^2 area of a membrane fiber sequentially immersed in pure water, a 1 mM, and then a 20 mM solution of CTAC. Processing the forces through that model, we estimated the number of molecules adsorbed on the cellulose fibers. The obtained values seem to be reasonable compared to the previously reported adsorption of similar surfactant on silica surface. The method can be applied to study molecular adsorption of virtually any molecules.

Acknowledgements

The authors acknowledge support of this work thorough CCE New Ideas Grant.

Notes and references

‡ **Corresponding author:** igor.sokolov@tufts.edu
The authors declare no competing financial interest.

1 U. Bilitewski, *Analytica Chimica Acta*, 2006, **568**, 232-247.
2 B. Maisch, E. Bauer, M. Cirsi and K. Kochsiek, *Circulation*, 1993, **87**, 49-65.
3 W. R. Bowen, J. I. Calvo and A. Hernandez, *J Membrane Sci*, 1995, **101**, 153-165.
4 C. Loderer, B. Gahleitner, K. Steinbacher, C. Stelzer and W. Fuchs, *Sep Purif Technol*, 2013, **120**, 410-414.
5 S. Chellam and N. G. Cogan, *J Membrane Sci*, 2011, **382**, 148-157.
6 A. Zydney and R. Van Reis, *J. Memb. Sci.*, 2007, **297**, 34.
7 I. H. El-Sayed, X. Huang and M. A. El-Sayed, *Nano Lett*, 2005, **5**, 829-834.
8 H. Elwing, *Biomaterials*, 1998, **19**, 397-406.
9 E. Tyrode, M. W. Rutland and C. D. Bain, *Journal of the American Chemical Society*, 2008, **130**, 17434-17445.
10 I. Sokolov, V. Subba-Rao and L. A. Luck, *Biophysical Journal*, 2006, **90**, 1055-1063.
11 H. Z. Chen, Y. C. Xiao and T. S. Chung, *Polymer*, 2010, **51**, 4077-4086.
12 D. Volkov, G. Strack, J. Halamek, E. Katz and I. Sokolov, *Nanotechnology*, 2010, **21**, 145503.
13 J. W. C. Cheung and G. C. Walker, *Langmuir*, 2008, **24**, 13842-13849.
14 Y. L. Lyubchenko, L. S. Shlyakhtenko and T. Ando, *Methods*, 2011, **54**, 274-283.
15 J. Yang, J. X. Mou and Z. F. Shao, *Febs Letters*, 1994, **338**, 89-92.
16 I. Sokolov, M. Firtel and G. S. Henderson, *Journal of Vac.Sci.&Tech. B*, 1996, **14**, 674-678.
17 Y. Kim, E. S. Kim, Y. Lee, J. H. Kim, B. C. Shim, S. M. Cho, J. S. Lee and J. W. Park, *J Am Chem Soc*, 2014, **136**, 13754-13760.
18 Y. Lee, S. H. Kwon, Y. Kim, J. B. Lee and J. W. Park, *Anal Chem*, 2013, **85**, 4045-4050.
19 S. A. Claridge, J. J. Schwartz and P. S. Weiss, *ACS Nano*, 2011, **5**, 693-729.
20 H. J. Butt, M. Kappl, H. Mueller, R. Raiteri, W. Meyer and J. Rühe, *Langmuir*, 1999, **15**, 2559-2565.
21 S. Garcia-Manyes and F. Sanz, *Biochim Biophys Acta*, 2010, DOI: S0005-2736(09)00438-6 [pii]
22 10.1016/j.bbamem.2009.12.019.
23 G. Francius, D. Alsteens, V. Dupres, S. Lebeer, S. De Keersmaecker, J. Vanderleyden, H. J. Gruber and Y. F. Dufrene, *Nat Protoc*, 2009, **4**, 939-946.
24 M. Rief, F. Oesterhelt, B. Heymann and H. E. Gaub, *Science*, 1997, **275**, 1295-1297.
25 I. Sokolov, M. E. Dokukin and N. V. Guz, *Methods*, 2013, **60**, 202-213.
26 I. Sokolov, S. Iyer, V. Subba-Rao, R. M. Gaikwad and C. D. Woodworth, *Applied Physics Letters*, 2007, **91**, 023902-023901-023903.
27 M. Radmacher, *Methods Cell Biol*, 2007, **83**, 347-372.
28 M. E. Dokukin, N. V. Guz and I. Sokolov, *Biophys J*, 2013, **104**, 2123-2131.
29 N. Guz, M. Dokukin, V. Kalaparthi and I. Sokolov, *Biophys J*, 2014, **107**, 564-575.
30 L. D. Landau, E. M. Lifshi*t*s, A. d. M. Kosevich and L. P. Pitaevski*i, *Theory of elasticity*, Pergamon Press, Oxford Oxfordshire ; New York, 3rd English edn., 1986.
31 J. N. Israelachvili and H. Wennerstrom, *J Phys Chem-Us*, 1992, **96**, 520-531.
32 J. Israelachivili, *Intermolecular and Surface Forces* Academic. Press, Burlington, MA, 3rd edn., 2011.
33 S. Iyer, R. M. Gaikwad, V. Subba-Rao, C. D. Woodworth and I. Sokolov, *Nature Nanotechnology*, 2009, **4**, 389-393.
34 R. M. Servuss and H. W., *J. Phys. France* 1989, **50**, 809 - 827.
35 J. Jimenez and R. Rajagopalan, *Langmuir*, 1998, **14**, 2598-2601.
36 R. M. Pashley and J. N. Israelachvili, *Colloid Surface*, 1981, **2**, 169-187.
37 I. Sokolov, Q. K. Ong, H. Shodiev, N. Chechik, D. James and M. Oliver, *Journal of colloid and interface science*, 2006, **300**, 475-481.
38 I. Sokolov, V. Kalaparthi, M. Kreshchuk and M. E. Dokukin, *Ultramicroscopy*, 2012, **121**, 16-24.
39 Z. V. Leonenko, E. Finot, H. Ma, T. E. S. Dahms and D. T. Cramb, *Biophysical Journal*, 2004, **86**, 3783-3793.
40 J. N. Israelachvili, *Intermolecular and Surface Forces, 3rd Edition*, 2011, DOI: 10.1016/B978-0-12-375182-9.10014-4, 291-340.
41 R. Atkin, V. S. J. Craig, E. J. Wanless and S. Biggs, *Journal of colloid and interface science*, 2003, **266**, 236-244.
42 H.-J. Butt and M. Kappl, *Introduction, in Surface and Interfacial Forces*, Wiley-VCH Verlag GmbH & Co. KGaA, Weinheim, Germany, 2010.
43 I. Sokolov, H. Yang, G. A. Ozin and G. S. Henderson, *Advanced Materials*, 1997, **9**, 917-921.